RSC Sustainability

ROYAL SOCIETY OF CHEMISTRY

PAPER

View Article Online
View Journal | View Issue

Cite this: *RSC Sustainability*, 2025, **3**, 1157

Towards flexible large-scale, environmentally sustainable methanol and ammonia co-production using industrial symbiosis†

Joshua Magson,[a] Thérèse G. Lee Chan,[b] Akeem Mohammed[b] and Keeran Ward *[a]

As industries face increasing societal and governmental pressures to adopt sustainable practices, the methanol (MeOH) and ammonia (NH_3) sectors, significant contributors to greenhouse gas (GHG) emissions, are seeking innovative solutions to transition toward net-zero emissions. Here, we report on the use of industrial symbiosis (IS) as a transformative strategy to facilitate the cleaner co-production of MeOH and NH_3 by integrating green hydrogen (H_2) within a carbon capture and utilisation (CCUS) flowsheet. We examined the environmental assessment of various co-production pathways across a system boundary, which includes three (3) leading technologies – Steam Methane Reforming (SMR), Autothermal Reforming (ATR) and Gas Heated Reforming (GHR), considering both business-as-usual (BAU) and hybrid IS integration (Hyd). MeOH flowsheets utilised all three technologies, while NH_3 production employed SMR and ATR systems. This comprised six (6) BAU MeOH and NH_3 co-production schemes (GHR–SMR_{BAU}, SMR–SMR_{BAU}, ATR–SMR_{BAU}, GHR–ATR_{BAU}, SMR–ATR_{BAU}, ATR–ATR_{BAU}) and six (6) Hyd (GHR–SMR_{Hyd}, SMR–SMR_{Hyd}, ATR–SMR_{Hyd}, GHR–ATR_{Hyd}, SMR–ATR_{Hyd}, ATR–ATR_{Hyd}) cases, utilising cradle-to-gate life cycle assessments (LCA). Results show that IS-integrated flowsheets reduced GHG emissions by 12–28% compared to BAU operations, with GHG impacts improving in the order GHR–ATR_{Hyd} > ATR–ATR_{Hyd} > SMR–ATR_{Hyd} > GHR–SMR_{BAU} > ATR–SMR_{BAU} > SMR–SMR_{BAU}, in agreement with energy and resource efficiency results. Notably, the GHR–ATR_{Hyd} configuration outperformed all other cases, reducing natural gas consumption by 11% and heating requirements by 8.3%. Furthermore, sustainability results support IS as a pathway to environmental benefits-with ATR-based NH_3 operations achieving up to 31% improved impacts linked to both ecosystem quality and human health. Ultimately, our study underscores the critical role of IS in advancing resilient, low-carbon practices, promoting sustainable technologies for net-zero emissions and defossilisation, thereby supporting a transformative shift towards sustainable industrial operations.

Received 16th October 2024
Accepted 17th December 2024

DOI: 10.1039/d4su00647j

rsc.li/rscsus

Sustainability spotlight

Methanol and ammonia are critically important building blocks for several commodities from solvents and fuels to fertilizers. Thus, defossilization at large scale is essential for cleaner production. While presently the two systems are treated independently, our study seeks to investigate industrial symbiosis as a pathway to sustainable coproduction schemes utilizing cleaner, advanced technologies and greener supply chains. Here, we modeled and examined the life cycle impacts of independent production *versus* integrated processing, highlighting the impact of increased process efficiency and reduced resource intensity in decreasing carbon footprint while acknowledging burden-shifting. Our results align directly to the UN sustainable development goals of industry, innovation and infrastructure (SDG 9), responsible consumption and production (SDG 12) and climate action (SDG 13).

1. Introduction

On a global scale, GHG emissions have increased by 50% over the last 30 years,[1] in which CO_2 emissions have increased from 22.75 billion tonnes per annum to 37.15 billion as of 2022 (63.3% increase). The Paris Agreement in 2015, amongst other legislations, set out the ambitious target to limit global temperature rises to 1.5 °C and decrease global GHG emissions by 43% by 2030.[2] However, current trends in emissions and

[a]*School of Chemical and Process Engineering (SCAPE), University of Leeds, Leeds, LS2 9JT, UK. E-mail: k.r.ward@leeds.ac.uk*

[b]*Department of Chemical Engineering, University of the West Indies, St. Augustine, WI, Trinidad*

† Electronic supplementary information (ESI) available: All specific data supporting this article have been included as part of the ESI. See DOI: https://doi.org/10.1039/d4su00647j

infrastructure put these commitments in jeopardy,[3] concluding that overall emissions within the chemical industry must be reduced by 60% to meet these targets.[4] As an initiative to reduce GHG emissions, chemical manufacturing companies have also agreed to cut emissions *via* more renewable chemical production routes, particularly weaning off the use of fossil fuel feedstocks. This is particularly apparent in the production of both MeOH and NH_3, which are predominantly produced from natural gas.

MeOH is considered to be one of the most important chemical raw materials and is even identified as playing an essential role in the transition from fossil fuels to renewable energy since it can be easily transported and has the potential to be an energy carrier for hydrogen storage.[5] Based on the current MeOH capacities, 90% is derived from natural gas feedstocks, predominantly *via* steam methane reforming (SMR), autothermal reforming (ATR) and gas-heated reforming (GHR) technology routes.[6] Globally, MeOH production has increased at a compound annual growth rate (CAGR) of 5.2%, resulting in the production rate exceeding 110 million MTPA in 2021.[1] This increasing MeOH demand has been driven by its versatility in its use as a feedstock in further chemical generation, including processing formaldehyde, acetic acid, dimethyl ether, gasoline blending and fuel cells.[7] On top of this, 40% of methanol consumption worldwide comprises energy-related uses.[8]

NH_3, like MeOH, is a necessary commodity chemical, and it is especially important in the fertiliser industry. It has also been identified as a liquid energy carrier, and therefore, it makes it a powerful option for fuel.[9] NH_3 is typically produced by steam methane reforming (SMR) of natural gas to produce hydrogen, which is then combined with nitrogen in the Haber–Bosch process. Like MeOH, the global consumption of NH_3 is expected to increase. In 2022, the global NH_3 market size was upwards of USD 202 billion and is projected to surpass USD 353.3 billion by 2032 (5.8% CAGR).[10] A worldwide intensification of agriculture primarily drives this expected growth to meet higher food demands for a rapidly increasing population, which is expected to double by 2050.[11] Due to this excessive use, NH_3 production releases more CO_2 into the atmosphere than any other large-scale chemical process and accounts for 1.8% of global GHG emissions.

It is evident that there is a high demand for both MeOH and NH_3, but since both are predominantly produced from natural gas, this leads to high GHG emissions, which is a significant downfall. MeOH and NH_3 production from natural gas *via* SMR emits 0.62 t CO_2e per t MeOH and 2.16–2.51 t CO_2e pet t NH_3 respectively.[12,13] Without changing the BAU operations, which have been mostly reliant on fossil fuels, it is expected that CO_2 emissions from MeOH production will rise to 1.5 Gt CO_2 per year by 2050.[14]

Co-production of MeOH and NH_3 allows for flexibility in plant operations and a decrease in natural gas usage. High-purity CO_2 from the NH_3 plants can be used as a feedstock for MeOH production *via* the CO_2 hydrogenation route, which has a lower thermal efficiency compared to conventional methods.[15] The co-production scheme not only enables production with overall decreased GHG emissions but creates industrial symbiotic linkages between the plants since the waste CO_2 from the NH_3 plant is used as a feedstock in the MeOH plant. The concept of industrial symbiosis (IS) is not new and has existed for more than three decades.[16] It is a concept where resource exchanges and the transactions amongst entities are mutually beneficial for all involved and has the potential to create a cyclic approach to production compared to a linear transformation from raw materials to production, thereby supporting a circular economy approach. Previous studies have shown that IS can reduce GHG emissions and CO_2 emissions and create an overall positive environmental impact.[17–20]

The waste emissions in the co-production scheme can be further reduced by considering alternative energy sources. For sustainable NH_3 production, biochemical pathways and water electrolysis using renewable sources have been investigated.[21] Similarly, multiple routes for sustainable MeOH production have been investigated, which also includes thermo-catalytic hydrogenation and biocatalysis.[22] However, the major challenge encountered is the technology readiness level (TRL) and economics associated with the alternative pathways compared to the BAU scenarios.[23] Green hydrogen (H_2) has shown promise and is deemed a suitable alternative to fossil-based fuels.[24] There are various pathways for green H_2 production which includes thermal, electrochemical and biological primary methods.[25] Thermal and electrolysis conversion pathways for H_2 production have been identified as the focal areas for research to achieve the targets of the production of 10 Mt of clean H_2 by 2030 and 50 Mt by 2050 based on the U.S. National Clean Hydrogen Strategy and Roadmap.[26] In 2022, the global H_2 demand was 95 Mt and was deemed as a historical high and it is estimated that this production accounted for greater than 900 Mt of CO_2 emissions since H_2 was produced mainly by traditional methods. Out of this demand, 50% was required for NH_3 and MeOH production and hence was responsible for 450 Mt of CO_2 emissions. In the United States, SMR currently accounts for the majority of the commercially produced H_2 (ref. 27) but the country has begun putting policies in place for cleaner H_2 production. In 2021, $9.5 billion was allocated for clean H_2 production and in 2022, additional policies and incentives were put in place to boost the country's market for H_2 production. However, it is not expected that clean H_2 production methods will completely replace the traditional approaches. Reasons for this include technological issues with H_2 production, distribution and storage,[28] high cost,[29] scarcity of resources for infrastructure development,[30] and the unreliability of renewable energy sources.[31]

Nevertheless, due to the high usage of H_2 in the NH_3 and MeOH sectors, it is anticipated that a fraction of the clean H_2 will be integrated into these sectors and would significantly reduce emissions for both production schemes. Based on the target clean H_2 production in the United States, it is expected that there will be a hybrid system using both clean H_2 and fossil-based H_2. Despite the continuous effort towards a low-carbon economy, little work has been done in investigating co-production schemes for commodities such as MeOH and NH_3 and the transition to a hybrid system using both fossil-based and green H_2. In this study, we examine the co-production of

MeOH and NH_3 using various technologies and the integration of green H_2 through LCAs. These results will assist in charting the way forward to lower GHG emissions and more sustainable operations.

2. Methodology

This section provides a detailed overview of the modelling framework, and scenario-specific descriptions applied to the integrated co-production of MeOH and NH_3, utilising IS. Our analysis considers validated process design, for which mass and energy balances were derived and used to inform life cycle assessments and energy and resource efficiencies.

2.1 Geographical process boundary

In the United States, the chemical and petrochemical industries which are mainly concentrated in the Gulf Coast, particularly in Texas and Louisiana, account for approximately 40% of industrial energy consumption and emissions.[32] Louisiana is renowned for its booming oil and gas and petrochemical sectors. The petrochemical sector houses more than 150 petrochemical plants and 15 refineries and is therefore a strategic location for process industries.[33] The majority of the plants are located in the St. James Parish along the lower Mississippi River corridor between Baton Rouge and New Orleans and is known as the Louisiana Chemical Corridor.[34,35] The state possesses the third highest energy consumption and the second highest energy consumption per capita in the United States. In 2022, approximately 4230 GW h of energy was generated with the leading sources being natural gas and nuclear power. Renewable energy from biomass, hydropower and solar energy accounted for 3.5% of the net electricity generation. Approximately 70% of the available energy is consumed by the industrial sector.[36] Although most of the energy is produced *via* natural gas, Louisiana is considering alternative energy sources such as solar and offshore wind. The climate in Louisiana is conducive to solar energy production since it has a high average of warm and sunny days compared to other states and flat, land space is available to install solar panels. Louisiana has the potential to generate up to 13 000 MW of solar power.[37] This amount of solar power is more than sufficient to provide green hydrogen for this project in Louisiana. Fig. 1 shows the approximate location of the existing chemical plants, and the system boundary used in this study.

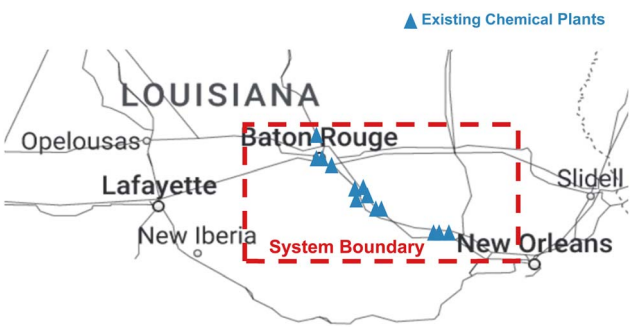

Fig. 1 Geographical boundary.

2.2. Process system overview

The overall process system boundary is given in Fig. 2. Technologies investigated considered validated large-scale SMR_{MeOH}, ATR_{MeOH} and GHR_{MeOH} reforming operations for MeOH production coupled with conventional SMR_{NH_3} and ATR_{NH_3} flowsheets for NH_3 manufacturing. Process inventories for all MeOH technologies and SMR_{NH_3} production were taken from our previous work,[1,38] which were validated against industrial data, while ATR_{NH_3} flowsheets were modelled using Aspen Plus (V10) process simulation software, utilising the RK-Aspen property package. ATR_{NH_3} was considered in this study since Air Liquide and KBR are partnering to develop NH_3 plants using this process.[39] Thus, our analysis compares six (6) business-as-usual (BAU) MeOH and NH_3 co-production schemes (GHR–SMR_{BAU}, SMR–SMR_{BAU}, ATR–SMR_{BAU}, GHR–ATR_{BAU}, SMR–ATR_{BAU}, ATR–ATR_{BAU}) and six (6) hybridised (Hyd) IS flowsheets (GHR–SMR_{Hyd}, SMR–SMR_{Hyd}, ATR–SMR_{Hyd}, GHR–ATR_{Hyd}, SMR–ATR_{Hyd}, ATR–ATR_{Hyd}). For BAU co-production schemes, conventional mega-methanol and NH_3 flowsheets operating at 5000 MTPD and 1850 MTPD, respectively, were considered as these scales were consistent with large-scale MeOH and NH_3 production. Several industry leaders, including Johnson Matthey, in conjunction with KBR, have already begun to examine the potential co-production of MeOH and NH_3. The proposed method of integration can produce up to approximately 6800 MTPD of MeOH and NH_3 combined, and it has been shown that this co-production is competitive with current industrial scales.[40]

Within the BAU co-production flowsheet, each technology was operated independently to produce both MeOH and NH_3 without IS. For integrated IS flowsheets, CO_2 flows from both SMR and ATR NH_3 operations were used to produce E-methanol embedded within MeOH process designs. The IS flows for each process are shown in Table 1. To promote flexible BAU MeOH operations, fossil-based production was ramped down to support E-methanol operations while maintaining large-scale capacity. Green H_2 feedstocks required for E-methanol production were derived from solar-powered PEM electrolysis, operating at an efficiency of 70.5%, a capacity factor of 0.241 and a standard enthalpy of electrolysis of 39 kW h per kg H_2.[41] The scale of E-methanol operations was constrained to 270 000 tonnes per year (Total capacity = 300 000 tonnes per year, on-stream factor assumed at 90%) in accordance with typical global E-methanol operations.[42] and the solar power resource capacities of the Louisiana region. As SMR MeOH technologies utilised CO_2 for combined steam and dry methane reforming, IS-integrated SMR–SMR_{Hyd} cases required external CO_2 feedstocks for co-production and, thus, captured CO_2 from natural gas power plant operations were utilised. Process inventories for E-methanol production and captured CO_2 were taken from the work by González-Garay *et al.*[41]

2.2.1 ATR_{NH_3} process development. The overall ATR_{NH_3} flowsheet is given in Fig. 3. The front-end plant model followed

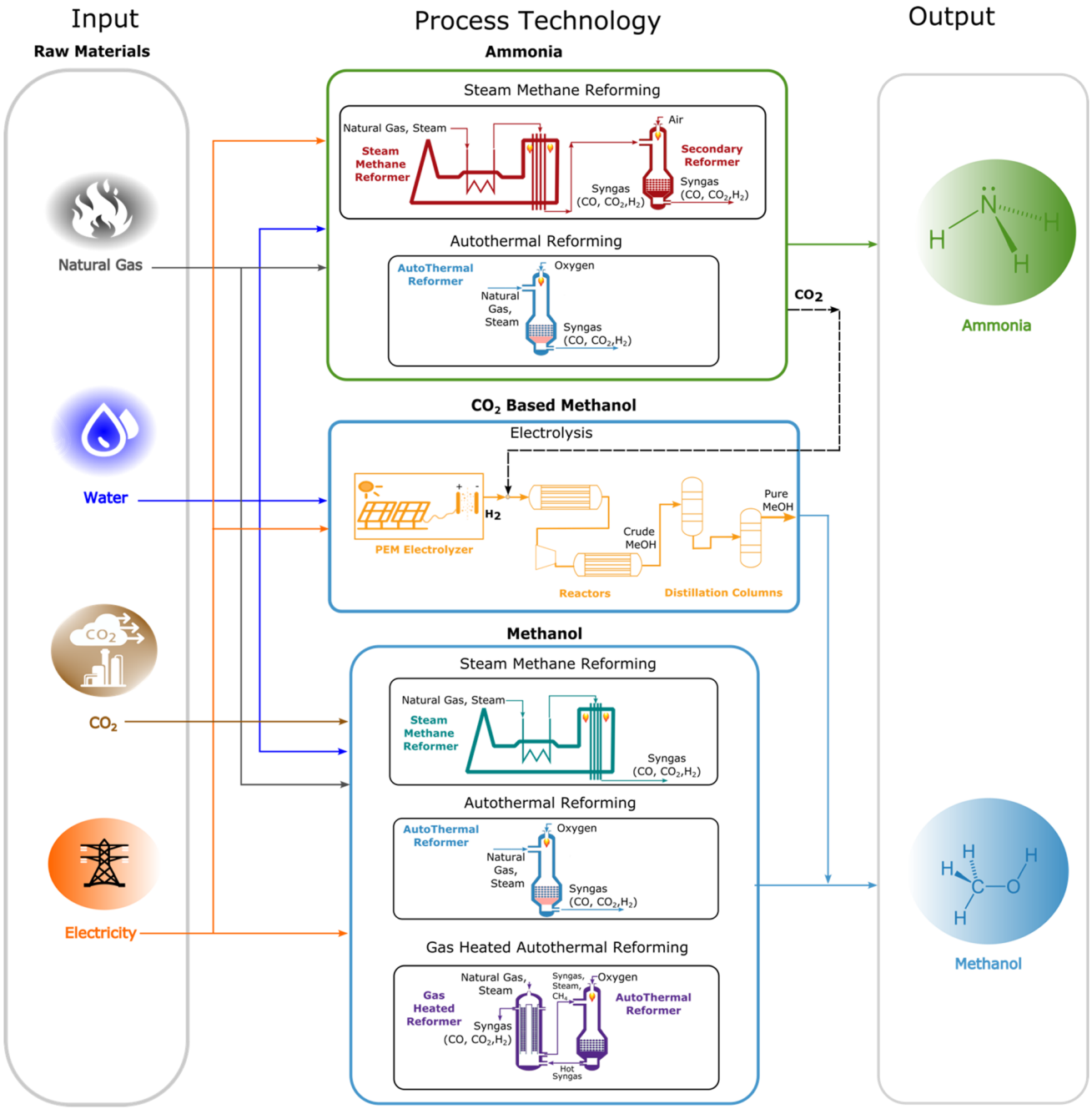

Fig. 2 Overall process system boundary. The system includes inputs in the form natural gas, water, CO_2, electricity, for cleaner co-production of MeOH and NH_3 by integrating green H_2 produced *via* solar powered electrolysis and captured CO_2 from NH_3 synthesis.

Table 1 IS flows associated with each process

Process/technology	Capacity [MTPD]	IS flows entering	IS flows exiting
SMR_{MeOH}	5000	CO_2	None
ATR_{MeOH}	5000	None	None
GHR_{MeOH}	5000	None	None
E-methanol	822	H_2, CO_2	None
SMR_{NH_3}	1850	None	CO_2
ATR_{NH_3}	1850	None	CO_2

standard ATR-based H_2 production according to available literature.[43,44] Desulphurised natural gas was compressed to 49 bar and mixed with medium-pressure (MP) steam at a steam-to-carbon ratio of 0.6. This mixed feed gas was preheated to pre-reforming conditions (480 °C), allowing for the methanation of higher hydrocarbons (eqn (1)–(4)), creating a lean methane-rich feed gas for autothermal reforming. The lean feed gas was mixed with preheated oxygen (99.5% mol, 300 °C) and reacted in an adiabatic ATR unit. Methane partial oxidation (eqn (6) and (7)) occurs simultaneously with reforming

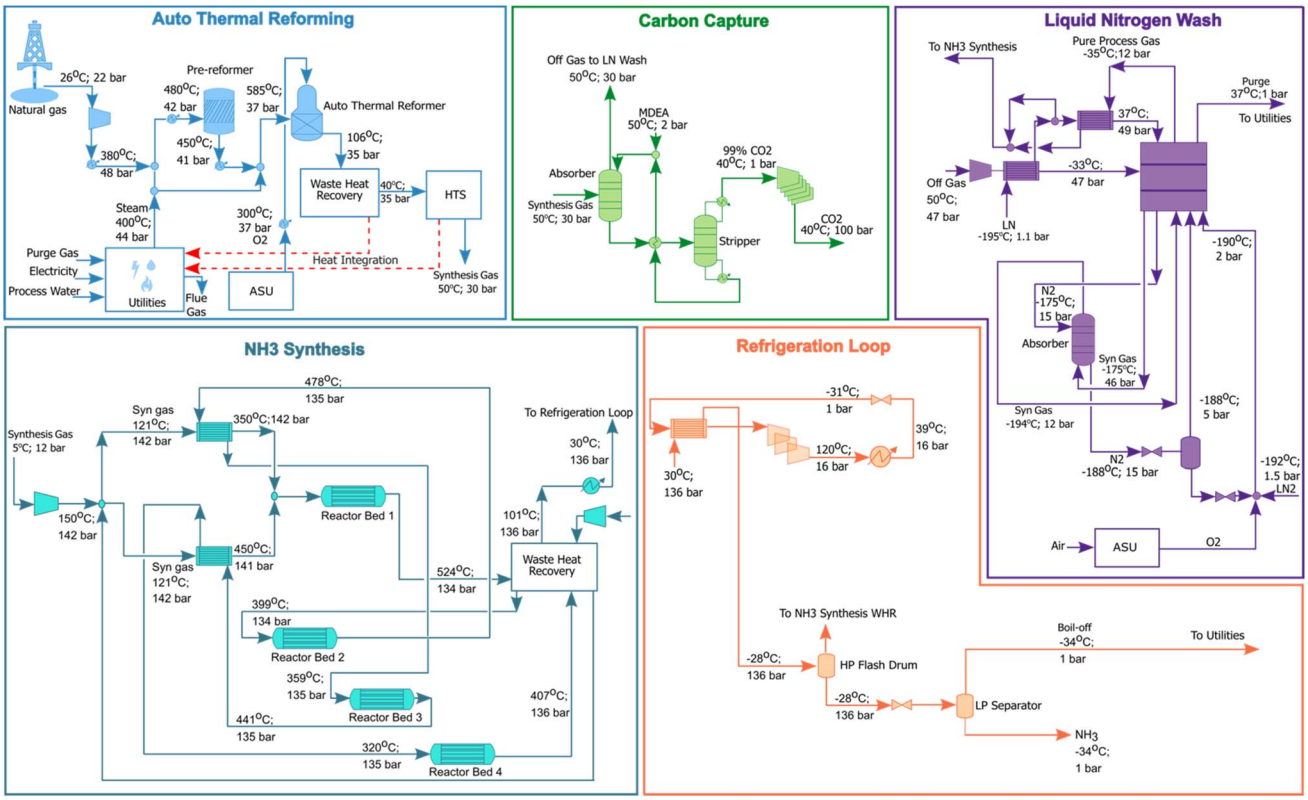

Fig. 3 Overall ATR_{NH_3} flowsheet consisting of five (5) unit operations, including auto-thermal reforming, carbon capture, liquid nitrogen wash, ammonia synthesis and product removal using refrigeration. Process integration is linked throughout, illustrating the transfer of purge gases and boil-off for energy recovery as well as heat recovery across synthesis and reforming sections.

reactions (eqn (4) and (5)), providing the thermal energy required for steam reforming. The hot reformed gas was then cooled through waste heat recovery, mixed with auxiliary MP steam and reacted across two high-temperature water–gas shift converters, where CO is converted into CO_2 (eqn (4)). The resulting H_2-rich gas was further cooled and sent to CO_2 removal.

$$C_2H_6 + 2H_2O \rightarrow 2CO + 5H_2,\ \Delta H = 346.6\ \text{kJ mol}^{-1} \quad (1)$$

$$C_3H_8 + 3H_2O \rightarrow 3CO + 7H_2,\ \Delta H = 499.0\ \text{kJ mol}^{-1} \quad (2)$$

$$CO + 3H_2 \leftrightarrow CH_4 + H_2O,\ \Delta H = -205.9\ \text{kJ mol}^{-1} \quad (3)$$

$$CO + H_2O \leftrightarrow CO_2 + H_2,\ \Delta H = -41.1\ \text{kJ mol}^{-1} \quad (4)$$

$$CH_4 + H_2O \leftrightarrow CO + 3H_2,\ \Delta H = 205.9\ \text{kJ mol}^{-1} \quad (5)$$

$$CH_4 + 2O_2 \rightarrow CO_2 + 2H_2O,\ \Delta H = -401.4\ \text{kJ mol}^{-1} \quad (6)$$

$$CH_4 + O_2 \rightarrow CO + H_2 + H_2O,\ \Delta H = -277.9\ \text{kJ mol}^{-1} \quad (7)$$

The CO_2 removal unit was modelled based on our past work,[7] assuming a rate-based methyl-diethanolamine (MDEA) capture system with a 90% capture efficiency and normalised heating and cooling demands of 5.7 and 6.2 kJ per kg CO_2. The sweet synthesis gas leaving the CO_2 removal unit was sent to an adsorber where residual CO_2 and moisture were removed. The dried synthesis gas is chilled to −175 °C through a triple cascade counter-current heat exchange system and washed with liquid nitrogen, where inerts are completely removed. The final purified gas was mixed with gaseous nitrogen, ensuring a 3 : 1 ratio of $H_2 : N_2$ required for NH_3 synthesis. The liquid nitrogen system was modelled using the conditions described by Haonan *et al.*[45]

The back end section of the ATR NH_3 flowsheet considered a traditional Haber–Bosch process,[46] whereby N_2 and H_2 react to produce NH_3 over an iron catalyst at 141 bar and 450 °C (eqn (8)). The NH_3 synthesis unit consists of 4 adiabatic-packed bed reactors, integrated with heat recovery and MP steam generation which effectively removes the heat of reaction. The reactor model followed Temkin and Pyzhev kinetics,[47] imported into Aspen Plus. The cooled effluent from the synthesis section was chilled to −33 °C using an NH_3 refrigeration cycle and flash separated at 1 bar to yield 100% pure product NH_3.

$$\tfrac{1}{2}N_2 + \tfrac{3}{2}H_2 \leftrightarrow NH_3,\ \Delta H = -45.6\ \text{kJ mol}^{-1} \quad (8)$$

The utilities section of the ATR process included heat recovery through steam generation, power generation, heating and cooling. Steam generated within the front and back end was used as feedstock for steam reforming and heating within CO_2

Table 2 Life cycle inventories for BAU and IS integrated (Hyd) MeOH–NH_3 co-production cases. Functional unit (FU) = 1 kg NH_3

Technology	GHR–SMR_{BAU}	SMR–SMR_{BAU}	ATR–SMR_{BAU}	GHR–ATR_{BAU}	SMR–ATR_{BAU}	ATR–ATR_{BAU}	GHR–SMR_{Hyd}	SMR–SMR_{Hyd}	ATR–SMR_{Hyd}	GHR–ATR_{Hyd}	SMR–ATR_{Hyd}	ATR–ATR_{Hyd}
Inputs-materials												
Natural gas[a] [kg]	2.37	2.65	2.55	1.96	2.24	2.14	2.14	2.37	2.29	1.73	1.97	1.88
Water [kg]	1.11	1.81	0.88	1.61	2.31	1.38	1.07	1.66	0.88	1.57	2.16	1.38
Captured CO_2[b] [kg]	—	—	—	—	—	—		1.41				
Green H_2 [kg]	—	—	—	—	—	—	0.089	0.089	0.089	0.089	0.089	0.089
Inputs-energy												
Electricity[c] [kW h]	1.10	0.20	0.27	1.35	0.45	0.52	1.07	0.31	0.37	1.31	0.56	0.62
Heating[d] [kW h]	4.69	11.22	5.37	—	6.53	0.68	4.69	10.15	5.26	—	5.46	0.57
Cooling [kW h]	6.49	9.09	8.09	5.66	8.26	7.26	6.37	8.55	7.70	5.54	7.71	6.87
Outputs-materials												
MeOH [kg]	2.71	2.71	2.71	2.71	2.71	2.71	2.71	2.71	2.71	2.71	2.71	2.71
NH_3 [kg]	1.00	1.00	1.00	1.00	1.00	1.00	1.00	1.00	1.00	1.00	1.00	1.00
Process CO_2 [kg]	1.23	0.34	1.23	1.47	0.58	1.47	0.56	—	0.56	0.80	0.06	0.80
Other CO_2 [kg]	1.22	2.88	1.71	0.19	1.85	0.68	1.26	2.64	1.67	0.23	1.61	0.64
Co-product allocation[e]												
MeOH	0.716	0.716	0.716	0.716	0.716	0.716	0.716	0.716	0.716	0.716	0.716	0.716
NH_3	0.284	0.284	0.284	0.284	0.284	0.284	0.284	0.284	0.284	0.284	0.284	0.284
KPIs[f]												
Energy efficiency [%]	66.93	61.51	63.72	79.59	72.05	75.12	67.31	62.68	64.58	80.14	73.65	76.32
Resource efficiency [MJ per $kg_{products}$]	31.28	35.00	33.71	25.89	29.61	28.31	31.13	34.24	33.16	25.74	28.85	27.76

[a] Total natural gas required both as feedstock and utility heating purposes. [b] Captured CO_2 from Natural Gas Power Plant. [c] Net electricity consumed considering total power generated within flowsheets. [d] Net heating consumed considering total heat produced from purge gas, NH_3 boil-off and total heat required by natural gas. [e] Economic allocation considering MeOH price = USD 0.679 kg^{-1},[48] NH_3 price = USD 0.73 kg^{-1}.[49] [f] Energy and resource efficiencies evaluated at LHV_{natgas} = 49 MJ kg^{-1};[50] LHV_{MeOH} = 22.7 MJ kg^{-1};[51] LHV_{NH_3} = 18.8 MJ kg^{-1};[52] LHV_{H_2} = 120.2 MJ kg^{-1}.[50]

removal and liquid nitrogen wash units. Purge gas arising from the liquid nitrogen wash and low-pressure NH_3 boil-off was combusted, providing heating duties within the front end and power generation for process operations, considering a standard Rankine cycle with an efficiency of 30%.

2.3 Life cycle assessment (LCA)

To investigate the environmental impacts associated with each scenario-specific co-production scheme, a cradle-to-gate LCA methodology was applied, utilising the ISO 14040:2006 framework. In accordance with the ISO framework, the assessment methodology is conducted across four (4) levels.

2.3.1 Level 1: goal and scope. The goal and scope of our study considers twelve (12) MeOH–NH_3 co-production system boundaries (Fig. 3), considering independent BAU MeOH and NH_3 co-production pathways as well as IS integrated schemes. As illustrated, CO_2 is the main IS flow, and it is combined with green H_2 to produce E-methanol, allowing for integrated waste-to-resource value chains. As the aim of our study is to examine climate-friendly NH_3 manufacturing, the functional unit was set as 1 kg NH_3 produced from each co-production scheme.

2.3.2 Level 2: life cycle inventory analysis (LCI). Scenario-specific inventories were defined from the integration of both technologies as described previously in Section 2.2, with foreground system inventories derived from literature data[1,38,41] and process simulations. In contrast, background supply chain inventories were taken from Ecoinvent databases. Economic allocation was used to distribute burdens between co-products, as neither system boundary expansion nor substitution were deemed favourable allocation approaches due to the complexity of the integrated flowsheets. The input–output structure is defined in Fig. 2, which illustrates the mass and energy flows for each technology. The inputs consisted of natural gas (both as a feedstock and utility), water, electricity, captured CO_2 and green H_2. Outputs were co-products of MeOH and NH_3, process-based (CO_2 removal in NH_3 technologies), and other CO_2 emissions arising from fuel combustion for heating and power generation within technologies. Detailed normalised inventories are given in Table 2 in the Results and discussion section.

2.3.3 Level 3: life cycle impact assessment (LCIA). In the LCIA stage of our study, both midpoint and endpoint characterisation methods were used, following the ReCiPe 2016 Hierarchist-H method, using SimaPRO LCA software. The Hierarchist (H) perspective method was deemed the most appropriate for our research, allowing for easier, quantitative comparison of the environmental burdens associated with each of our cases.[53] While the ReCiPe (H) midpoint characterisation considers 18 impact categories, only GHG missions (Global Warming Potential) were investigated for our study. However, to analyse the impact of potential burden-shifting within impact categories, endpoint characterisation was examined across three main areas-human health, ecosystem quality and resource depletion. The full LCIA results of all cases are given in ESI, Section 2.†

2.3.4 Level 4: interpretation. By comprehensively analysing the LCIA at both the midpoint and endpoint, decision variables can be used to compare BAU co-production schemes with IS-integrated flowsheets through multiple decision-making criteria (see Results and discussion section 3.4), guiding achieving cleaner large-scale NH_3 manufacturing.

3. Results and discussion

This section presents the results summary and analysis over five (5) main sections: LCI overview and Analysis, Energy and Resource Performance, LCIA, and Multiple Decision-Making Criteria. Twelve (12) MeOH and NH_3 co-production schemes were modelled and defined by mass and energy balances, correlated by key performance indicators and characterised by thermodynamic profiles and environmental burden quantification. By analysing hotspots and trade-offs within each case-specific model, multiple decision-making criteria were applied, revealing the most environmentally sustainable route to eco-friendly NH_3 production at scale.

3.1 LCI overview and analysis

Considering the overall performance of each technology, Table 2 gives an overview of the normalised mass and energy balance profiles for both BAU and IS-integrated (Hyd) co-production flowsheets. Focusing on BAU processes across all cases, SMR_{NH_3} technologies utilise, on average, approximately 17% more natural gas input and three times as much heat than ATR_{NH_3} cases. This is mainly attributed to the heating needs of SMR operations, both for primary and secondary reforming and steam production within both MeOH and NH_3 production. Looking closely at individual operations, ATR_{NH_3} utilise 40% more water than SMR_{NH_3} cases due to the increase in CO shift conversion arising from autothermal reforming and partial oxidation but requires 41% less cooling needs due to efficient heat recovery. Although ATR_{NH_3} flowsheets produce 20% more process CO_2 than SMR_{NH_3} operations, they require no additional heating needs, and thus, this increase in energy efficiency accompanies a 33% reduction in total CO_2 produced. Overall, NH_3 technologies consume less electricity than MeOH technologies, such as GHR units, where trade-offs between heating and electrification are required for pumping and compression. For IS integrated flowsheets, the inherent flexibility of MeOH operations accompanied reductions in natural gas utilisation (11%) and heating (8.3%) but an 8% increase in electricity consumption due to E-methanol operations. This decrease in the use of resources coupled with CO_2 utilisation saw an average 28% reduction in total CO_2 emissions across all IS cases compared to BAU operations. Ultimately, trade-offs between electrification and heating pose the greatest benefits in contributing to low-carbon NH_3 production, with the GHR–ATR_{Hyd} boasting net zero heating and the lowest recorded natural gas usage, cooling duties and total CO_2 emissions across all co-production cases.

3.2 Energy and resource efficiencies

The process performance of all co-production cases was analysed using energy efficiency (EE) and resource intensity (RI) KPIs, given in eqn (9) and (10) below:

$$EE = \frac{\sum_{p}^{n} F_p NHV_p}{\sum_{i}^{n} F_i NHV_i + E_{Grid}} \quad (9)$$

$$RI = \frac{F_{Natgas} NHV_{Natgas}}{\sum_{p}^{n} F_p} \quad (10)$$

where, $F_{i,p,Natgas}$ is the mass flow (kg s^{-1}) of raw materials, products, natural gas, $NHV_{i,p,natgas}$ is the heating value of raw materials, products, natural gas, E_{Grid} is the electricity consumption from the Louisiana power grid.

EE of a given process outlines the energy conversion rate from inputs to outputs, while RI shows the use of fossil fuel resources in producing both MeOH and NH_3. Thus, an increase in EE and a decrease in RI give a more energetically and resource-efficient process flowsheet, favouring greater sustainable operations. The results of EE and RI across all cases are presented in Fig. 4. In alignment with the process systems overviews provided in Section 3.1, general trends show EE increases and RI decreases in the order GHR > ATR > SMR, with ATR_{NH_3} technologies outperforming SMR_{NH_3} cases. Focusing on BAU flowsheets, SMR–SMR_{BAU} gives the highest RI and lowest EE at 35 MJ $kg_{Product}^{-1}$ and 61.5%, respectively. In contrast, GHR–ATR_{BAU} was the most energetically favourable at an RI of 25.89 MJ $kg_{Product}^{-1}$ and EE at 79.6%. Comparing like-for-like MeOH technologies across NH_3 flowsheets, EE improves between 17.1–19%, and RI decreases between 15.3–17.2% with the adoption of ATR_{NH_3} production. Similar results are observed considering hybrid operations, with GHR–ATR_{Hyd} operations outperforming all other cases at an EE of 80.1% and RI at 25.74 MJ $kg_{Product}^{-1}$. Notably, hybrid flowsheets do not suffer much energy penalties, with EE increasing within the range of 0.58–1.9% compared to BAU processes. This indicates the synergy between both flowsheets to support co-production. Although IS provides pathways towards efficient energy utilisation, it is important to note that GHR–ATR_{BAU} systems outperform all other cases except its own hybrid flowsheet GHR–ATR_{Hyd} – at most a 30% increase in EE and a 27% decrease in RI, promoting the need for greater energy analysis and trade-off assessment in co-production schemes.

3.3 LCIA

3.3.1 GHG impact. The LCIA results are given for different IS-integrated MeOH–NH_3 co-production flowsheets and BAU processes as outlined in Fig. 5. For BAU co-production schemes, the main hotspots identified were linked to natural gas consumption (22–26%) and direct CO_2 emissions (process + other) arising from co-production operations (53–75%). Minor GHG contributions cumulating 3–27% were attributed to electricity and water consumption. For all inventories, environmental burdens arise from releasing CO_2, CH_4 and N_2O across raw material supply chains, consistent with raw material extraction and processing, fossil fuel consumption and fugitive emissions. Across BAU cases, SMR_{NH_3} technologies performed worse than ATR_{NH_3}, with the highest GHG burdens of 1.23 kg CO_2e per kg NH3 assigned to SMR–SMR_{BAU} co-production. At the same time, the most significant reduction in GHG (28%) was observed for GHR–SMR_{BAU}, mainly due to lower direct CO_2 emissions associated with GHR operations.

Similar results were observed across hybrid co-production cases, with the main hotspots, natural gas consumption (22–26%) and direct CO_2 contributions (38–65%), being marginally lower. Furthermore, the addition of green H_2 and captured CO_2 added little to the overall GHG impact (1.1–11%), as consolidated impacts were heavily outweighed by reduced GHG burdens due to decreased natural gas utilisation and minimised process-based CO_2 emissions. Although overall performance followed similar trends at the BAU level, hybrid cases produced 12% less GHG emissions on average than BAU cases – with GHR–ATR_{Hyd} performing the best (0.76 kg CO_2e per kg NH_3). Notably, despite the apparent benefits of IS, hybrid SMR_{NH_3}

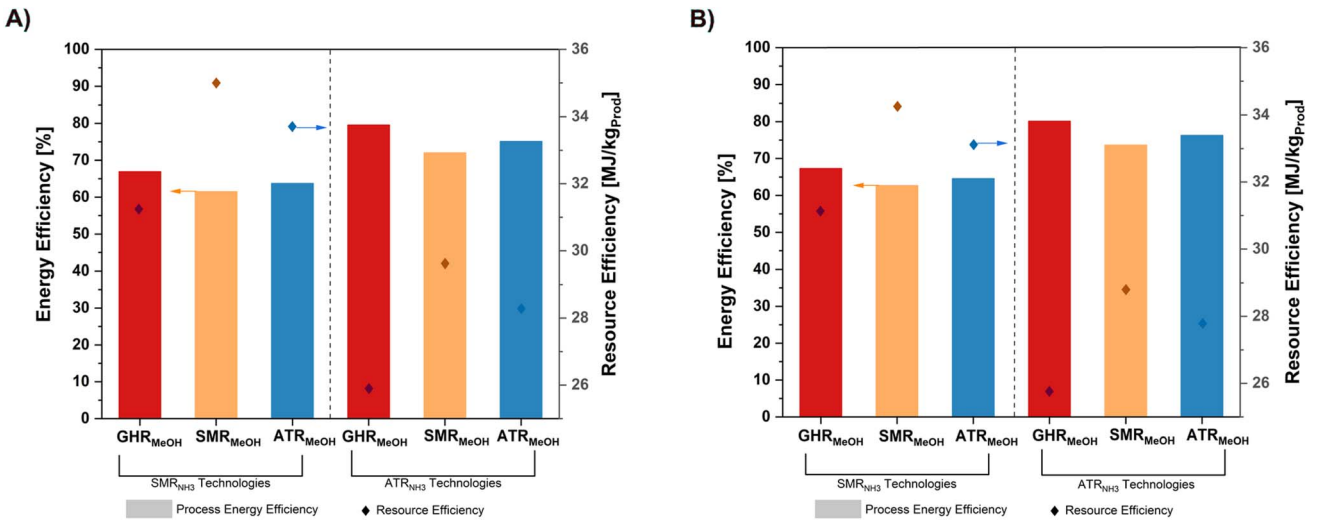

Fig. 4 Energy and resource efficiencies. (A) BAU cases, (B) IS integrated (Hyd) cases.

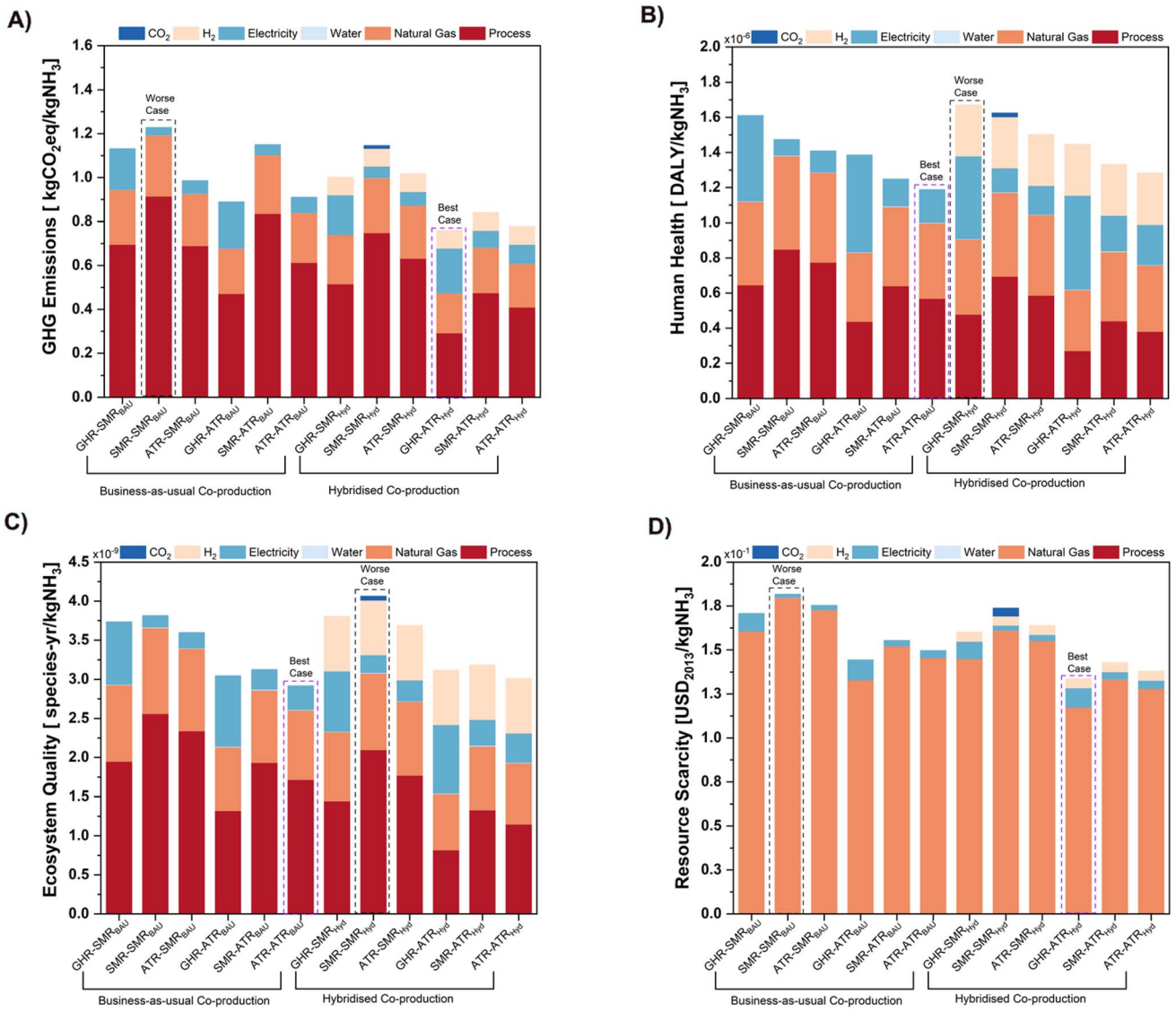

Fig. 5 LCIA results for all co-production cases across four (4) main categories including, (A) GHG emissions, (B) human health, (C) ecosystem quality and (D) resource scarcity.

technologies' GHG burdens exceeded ATR_{NH_3} BAU cases, illustrating the need to move towards ATR-based ammonia operations. Ultimately, GHG impacts improve in the order GHR–ATR_{Hyd} >ATR–ATR_{Hyd} > SMR–ATR_{Hyd} > GHR–SMR_{BAU} > ATR–SMR_{BAU} > SMR–SMR_{BAU}, in agreement with energy and resource efficiency results. While IS benefits are only realised through the integration of green H_2, the flexibility of IS-integrated co-production flowsheets will likely support larger E-methanol integration as renewable electricity is scaled up, allowing for greater sustainable operations of MeOH and NH_3 manufacturing.

3.3.2 Burden-shifting analysis. As IS supports decreased GHG impacts and resource intensities at the co-production level, it may accompany burden-shifting to other impact categories compared to BAU operations due to the integration of new feedstocks. Considering all midpoint categories (see ESI , Section 2†), burden-shifting is apparent across most impact categories, including ionising radiation, ozone formation, particulate matter, ecotoxicities, acidification, eutrophication, fossil resource scarcity and water consumption. At the endpoint, impacts were consolidated with human health burdens linked to particulate matter, ecotoxicities, ozone depletion, eutrophication, and acidification attributed to ecosystem quality. In contrast, global warming, ionising radiation and particulate matter are shared. Burdens affiliated with water consumption, fossil and mineral depletion and land usage are linked to resource scarcity. These burdens were mainly attributed to mining and mineral extraction, as well as materials production and fabrication, which released harmful compounds such as copper, zinc, antimony, lead, and arsenic, as well as radioactive sources, nitrogen oxides, phosphates and SO_2 into the environment. Focusing on endpoint impacts (Fig. 5(B and C)), burdens associated with natural gas consumption were reduced by 11%, moving away from BAU

operations – with improved IS contributions to human health and ecosystem quality ranging from 26–31% and 23–26%, respectively. These results were particularly noticeable in resource scarcity, where natural gas consumption dominated the burden contribution, ranging from 88–99%. Unlike the other endpoint impact categories, burden-shifting was not observed in resource scarcity – with technological performance following the same trends as described for GHG impact (best case, GHR–ATR_{Hyd} = 0.133 USD_{2013} per kg NH_3; Worse case, SMR–SMR_{BAU} = 0.182 USD_{2013} per kg NH_3). However, additional E-methanol operations worsen human health and ecosystem quality burdens, with green H_2 and increased electricity consumption leading to an increase in human health and ecosystem quality by 7% and 3%, respectively. Overall, ATR flowsheets performed the best across both human health (ATR–ATR_{BAU} = 1.19×10^{-6} DALY per kg NH_3) and ecosystem quality (ATR–ATR_{BAU} = 2.91×10^{-9} species-year per kg NH_3) and while GHR and SMR technologies performed the worse (GHR–SMR_{Hyd} = 1.67×10^{-6} DALY per kgNH_3; SMR–SMR_{Hyd} = 4.06×10^{-9} species-year per kg NH_3).

3.4 Multiple decision-making criteria

Normalised spider plots, as shown in Fig. 6, were developed to assist in a multi-criteria decision-making approach for evaluating the sustainability of the co-production systems. The indicators, which consisted equal weights of both environmental and process, were resource scarcity, ecosystem quality, human health, GHG emissions and process efficiency. The reverse score was used for process efficiency since this indicator should be maximised, compared to all the other indicators, which should be minimised. Therefore, the largest area in the normalised spider plots will represent the most inferior co-production system.

Focusing on BAU operations, where there are no IS linkages among processes, the SMR_{NH_3} cases were consistently outperformed due to higher burdens linked to all indicators. Although SMR is one of the most common and widely used methods for H_2 production for MeOH and NH_3 production,[54] our results illustrate that ATR alternatives produce more sustainable pathways, even if fossil-based natural gas is utilised. The GHR–ATR_{BAU} is the most compelling co-production system to utilise if using a system with only fossil-based fuels.

When IS linkages with CO_2 and H_2 were introduced to BAU production, there was a noticeable shift towards lower GHG emissions and resource scarcity and higher efficiency indicators for all the pathways as the integration of green H_2 and CO_2 reuse reduces the dependency of the fossil-based fuels without losing MeOH and NH_3 productivity. The most attractive co-production scheme using IS and green H_2 was the GHR–ATR_{Hyd} system while ATR–ATR_{Hyd} flowsheets show strong competitiveness as burden-shifting is reduced. Implementation of the GHR–ATR_{Hyd} system can lead to high process and resource efficiency and there would be a reduction in the overall GHG emissions compared to traditional systems where SMR technology is used. However, if existing industrial plants were retrofitted with these technologies, significant capital expenditure and the development of hydrogen production plants would be required and hence limit the implementation of the system. It should be noted that this system has shown to be best-performing co-production system compared to other systems, but these findings are valid only at the capacities considered in the study. Therefore, lower scale production systems may not show the same findings. Overall, our results illustrate the need for cleaner supply chains (*e.g.* renewable energy) within co-production schemes with IS as pathways to sustainable, large-scale production of MeOH and NH_3.

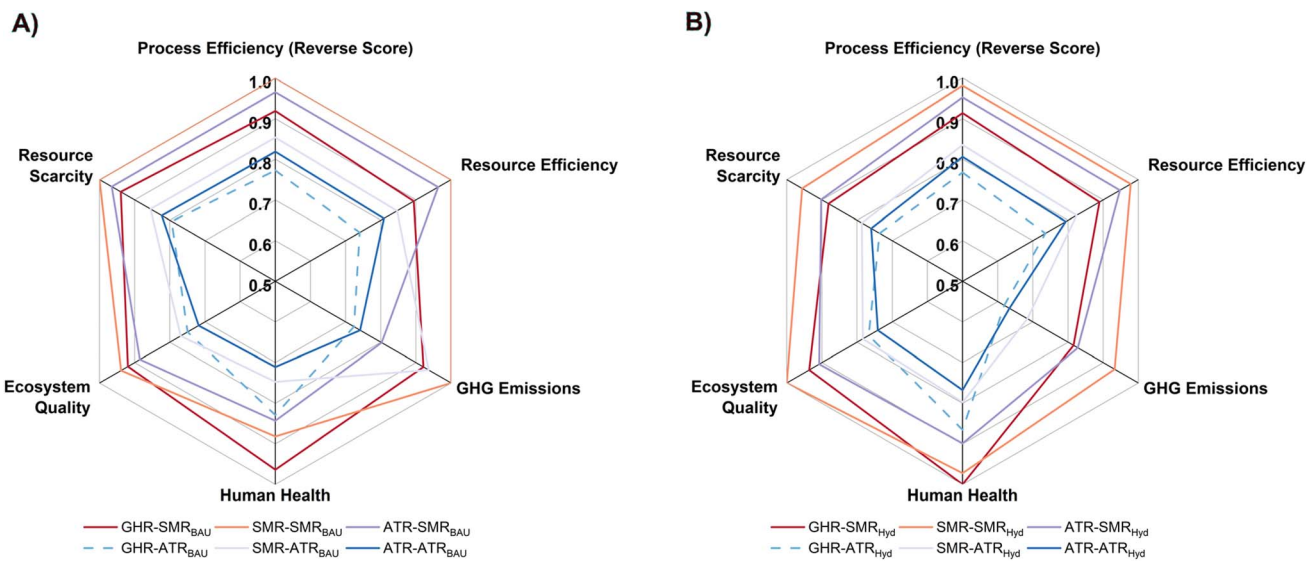

Fig. 6 Sustainability analysis of (A) BAU and (B) IS integrated MeOH–NH_3 co-production flowsheets. The blue dashed line [--] in both spider plots indicates the best-performing co-production flowsheet, which meets all decision criteria. This flowsheet was chosen as it has the smallest internal area and, thus, provides optimum results.

To achieve higher levels of IS and sustainability, companies must be willing to work together to develop these co-production systems. Although IS can be adopted using a top-down approach, it is recommended that companies employ a bottom-up approach where there is self-organisation of the IS exchanges amongst the plants. A recent example of self-organisation of IS for the co-production of MeOH and NH_3 is the partnership between KBR and Johnson Matthey.[40] This exemplifies that companies can successfully collaborate to achieve lower emissions and higher sustainability levels for their companies. As with all IS relationships, there are challenges involved which include technology readiness and maturity, economic factors and policy development.[55] However, if the companies have common goals of increasing sustainability levels and have the financial resources, these relationships can be nurtured and can flourish.

Further work can therefore be undertaken utilising supply chain optimisation of the co-production schemes with techno-economic analyses to highlight the viability of IS integration and hybridisation within conventional large-scale chemical production.

4. Conclusion

The inherent flexibility of IS-integrated co-production systems, which allow for seamless incorporation of renewable energy sources, positions them as pivotal players in the transition toward sustainable industrial practices. Our study underscores the transformative potential of IS in reshaping production within the existing MeOH and NH_3 industries. By integrating green H_2 produced through electrolysis and utilising CO_2 from NH_3 synthesis, we have demonstrated a viable pathway for significantly reducing the carbon footprint of these essential chemical industries. A detailed analysis revealed that the application of IS, mainly through the ATR_{NH_3} configurations, has shown superior performance in energy efficiency and reduced resource intensity compared to conventional SMR_{NH_3} systems. In contrast, IS-integrated flowsheets for MeOH demonstrate significant reductions in natural gas use and heating requirements albeit with an 8% increase in electricity consumption due to E-methanol production. These changes result in an average 28% reduction in total CO_2 emissions across IS cases compared to BAU operations. Notably, the trade-offs between electrification and heating offer substantial benefits for low-carbon NH_3 production, with the GHR–ATR_{Hyd} configuration achieving a noteworthy reduction in natural gas consumption and CO_2 emissions, highlighting its potential as a leading approach for low-carbon chemical manufacturing.

General trends indicate that EE increases and RI decreases in the order of GHR > ATR > SMR, with ATR_{NH_3} outperforming SMR_{NH_3} in most metrics. Specifically, the GHR–ATR_{BAU} configuration emerges as the most energetically favourable. While IS promotes efficient energy use, it is crucial to recognise that the GHR–ATR_{BAU} systems excel beyond other configurations, except for its hybrid variant GHR–ATR_{Hyd}. This underscores the necessity for comprehensive energy analysis and trade-off assessments in co-production schemes. In BAU co-production setups, the primary hotspots are linked to natural gas consumption and direct CO_2 emissions, with similar trends observed in hybrid systems, albeit with slightly lower impacts. GHG impacts improve in the sequence GHR–ATR_{Hyd} > ATR–ATR_{Hyd} > SMR–ATR_{Hyd} > GHR–SMR_{BAU} > ATR–SMR_{BAU} > SMR–SMR_{BAU}, aligning with energy and resource efficiency results. Although the benefits of IS are primarily realised through green H_2 integration, the inherent flexibility of IS-integrated co-production flowsheets supports greater E-methanol integration as renewable electricity scales up, enabling more sustainable MeOH and NH_3 production.

Looking ahead, future work offers significant opportunities to optimize IS-integrated systems and advance their sustainability. Building on the demonstrated environmental benefits of the IS pathway, key areas of focus include integrating GHR ammonia systems to explore additional low-carbon co-production schemes and conducting techno-economic analyses to assess their scalability and financial feasibility. Supply chain optimization processes can also be employed to determine the optimal mix of technologies and address logistical challenges, while incorporating life cycle costing will provide a comprehensive assessment of long-term economic and environmental impacts. Furthermore, identifying and addressing potential technical bottlenecks, such as process inefficiencies or material compatibility issues, will be critical. These efforts, combined with strategies to scale and commercialize IS systems, will help bridge the gap between research and industrial application, ultimately supporting broader absolute sustainability goals.

Overall, ATR configurations demonstrate superior performance across human health and ecosystem quality, whereas GHR and SMR technologies show less favourable outcomes. Despite potential burden shifting, the overall impact remains positive, with the GHR–ATR_{Hyd} approach emerging as the most favourable production method compared to current BAU processes - advancing decarbonisation efforts within the MeOH and NH_3 industries. Ultimately, this study demonstrates that IS is a viable strategy for the cleaner co-production of MeOH and NH_3, offering a transferable model for sustainable chemical production in other carbon-intensive industries, advocating for a promising pathway toward achieving net-zero emissions and defossilising chemical sectors.

Data availability

All specific data supporting this article have been included as part of the ESI.†

Conflicts of interest

There are no conflicts to declare.

Acknowledgements

The UK's Engineering and Physical Sciences Research Council (EPSRC) is acknowledged for the use of the SimaPro license at

The University of Leeds through the two grants EP/L014912/1 (CDT Bioenergy) and EP/T033088/1 (SusLABB).

References

1 J. Mahabir, N. Samaroo, M. Janardhanan and K. Ward, *J. CO_2 Util.*, 2022, **66**, 102302.
2 UNCC, What is the Paris Agreement?, **https://unfccc.int/process-and-meetings/the-paris-agreement**, accessed 19/07/2024.
3 W. Lamb F, T. Wiedmann, J. Pongratz, R. Andrew, M. Crippa, J. Oliver, G. J, D. Widenhofer, G. Mattiol, A. Khourdajie and J. House, *Environ. Res. Lett.*, 2021, **16**, 073005.
4 R. Cao, K. Lueck, C. Musso and V. Sarathy, The Chemicals Industry of Tomorrow: Collaborate to Innovate, **https://www.mckinsey.com/industries/chemicals/our-insights/the-chemicals-industry-of-tomorrow-collaborate-to-innovate**, accessed 02/04/2024.
5 F. Dalena, A. Senatore, A. Marino, A. Gordano, M. Basile and A. Basile, in *Methanol*, ed. A. Basile and F. Dalena, Elsevier, 2018, pp. 3–28, DOI: **10.1016/B978-0-444-63903-5.00001-7**.
6 S. A. Bhat and J. Sadhukhan, *AIChE J.*, 2009, **55**, 408–422.
7 K. Narine, J. Mahabir, N. Koylass, N. Samaroo, S. Singh-Gryzbon, A. Baboolal, M. Guo and K. Ward, *J. CO_2 Util.*, 2021, **44**, 101399.
8 T. Klein, *Methanol: A Future-Proof Fuel*, Future Fuel Strategies, 2020.
9 D. R. MacFarlane, P. V. Cherepanov, J. Choi, B. H. R. Suryanto, R. Y. Hodgetts, J. M. Bakker, F. M. Ferrero Vallana and A. N. Simonov, *Joule*, 2020, **4**, 1186–1205.
10 Precedence Research, Ammonia Market (By Product Form: Liquid, Gas, Powder; By Application: Fertilizers, Refrigerants, Pharmaceuticals, Textile, Others) - Global Industry Analysis, Size, Share, Growth, Trends, Regional Outlook, and Forecast 2023-2032, **https://www.precedenceresearch.com/ammonia-market**, accessed 04/11/2023.
11 H. Bouaboula, M. Ouikhalfan, I. Saadoune, J. Chaouki, A. Zaabout and Y. Belmabkhout, *Energy Rep.*, 2023, **9**, 4507–4517.
12 A. O. Oni, T. Giwa, C. Font-Palma and D. A. Fadare, *Int. J. Greenhouse Gas Control*, 2023, **123**, 103819.
13 S. Ghavam, M. Vahdati, I. A. G. Wilson and P. Styring, *Front. Energy Res.*, 2021, **9**, 580808.
14 IRENA and MI, *Innovation Outlook: Renewable Methanol*, International Renewable Energy Authority, Abu Dhabi, 2021.
15 Y. Khojasteh-Salkuyeh, O. Ashrafi, E. Mostafavi and P. Navarri, *J. CO2 Util.*, 2021, **50**, 101608.
16 R. A. Frosch and N. E. Gallopoulos, *Sci. Am.*, 1989, **261**, 144–153.
17 A. Wolf and M. Wallén, *Prog. Ind. Ecol.*, 2008, **5**, 502–517.
18 M. Martin, *J. Ind. Ecol.*, 2019, **24**, 626–638.
19 A. Neves, R. Godina, S. G. Azevedo and J. C. O. Matias, *J. Clean Prod.*, 2020, **247**, 119113.
20 T. G. Lee Chan and D. A. Janes, *Carbon Capture Sci. Technol.*, 2023, **7**, 100109.
21 S. C. D'Angelo, S. Cobo, V. Tulus, A. Nabera, A. J. Martín, J. Pérez-Ramírez and G. Guillén-Gosálbez, *ACS Sustain. Chem. Eng.*, 2021, **9**, 9740–9749.
22 A. Crivellari, V. Casson Moreno, V. Cozzani and I. Dincer, *J. Cleaner Prod.*, 2021, **293**, 126226.
23 A. Valera-Medina, F. Amer-Hatem, A. K. Azad, I. C. Dedoussi, M. de Joannon, R. X. Fernandes, P. Glarborg, H. Hashemi, X. He, S. Mashruk, J. McGowan, C. Mounaim-Rouselle, A. Ortiz-Prado, A. Ortiz-Valera, I. Rossetti, B. Shu, M. Yehia, H. Xiao and M. Costa, *Energy Fuels*, 2021, **35**, 6964–7029.
24 S. E. Hosseini and M. A. Wahid, *Int. J. Energy Res.*, 2020, **44**, 4110–4131.
25 T. I. Sigfusson, *Philos. Trans. R. Soc., A*, 2007, **365**, 1025–1042.
26 U.S. Department of Energy, *U.S. National Clean Hydrogen Strategy and Roadmap*, 2023, **https://www.hydrogen.energy.gov/pdfs/us-national-clean-hydrogen-strategy-roadmap.pdf**.
27 EIA, Production of Hydrogen, **https://www.eia.gov/energyexplained/hydrogen/production-of-hydrogen.php**, accessed 25/07/2024.
28 N. Armaroli and V. Balzani, *ChemSusChem*, 2011, **4**, 21–36.
29 W. Flood, *Energy Environ.*, 2012, **23**, 1097–1104.
30 R. Kleijn and E. van der Voet, *Renew. Sustain. Energy Rev.*, 2010, **14**, 2784–2795.
31 J. Flaig, 5 major challenges in the hydrogen economy in 2024 – and 5 potential solutions, **https://www.imeche.org/news/news-article/5-major-challenges-in-the-hydrogen-economy-in-2024-and-5-potential-solutions#:~:text=Ofthemajorchallengesin,to9.8TWhby2035**, accessed 26/07/2024.
32 Office of Energy Efficiency & Renewable Energy, Chemical and Petrochemical Manufacturing, **https://www.energy.gov/eere/iedo/chemical-and-petrochemical-manufacturing**.
33 Louisiana Economic Development, Process Industries, **https://www.opportunitylouisiana.gov/key-industry/process-industries**, accessed 17/07/2024.
34 A. D. Blodgett, *Local Environ.*, 2006, **11**, 647–661.
35 B. F. Snyder, M. Layne and D. E. Dismukes, *Int. J. Greenh. Gas Control*, 2020, **93**, 102885.
36 U.S. Energy Information Administration, *Annual Energy Outlook*, 2023, Retrieved 17/07/2024, from **https://www.eia.gov/outlooks/aeo/**.
37 Louisiana Economic Development, Louisiana Solar Power Generation is Growing, **https://www.opportunitylouisiana.gov/key-industry/energy/energy-diversity/solar**, accessed 18/07/2024.
38 N. Samaroo, N. Koylass, M. Guo and K. Ward, *Green Chem.*, 2020, **22**, 6547–6559.
39 A. Liquide, Air Liquide and KBR to offer ATR-based low-carbon ammonia and hydrogen technologies, **https://www.airliquide.com/group/press-releases-news/2023-07-19/air-liquide-and-kbr-offer-atr-based-low-carbon-ammonia-and-hydrogen-technologies**, accessed November 7, 2024.
40 J. Matthey, Methanol and ammonia co-production, **https://matthey.com/products-and-markets/chemicals/methanol/**

methanol-and-ammonia-co-production, accessed November 4, 2023.
41 A. González-Garay, M. S. Frei, A. Al-Qahtani, C. Mondelli, G. Guillén-Gosálbez and J. Pérez-Ramírez, *Energy Environ. Sci.*, 2019, **12**, 3425–3436.
42 M. Institute, Renewable Methanol, https://www.methanol.org/renewable/, accessed July 2, 2024.
43 Topsoe, SynCOR Ammonia™ – New process for grassroots plants, https://www.topsoe.com/our-resources/knowledge/our-products/process-licensing/syncor-ammoniatm-new-process-for-grassroots-plants, accessed July 3, 2024.
44 P. J. Dahl, SynCOR HydrogenTM The Optimal Solution for Blue, https://globalsyngas.org/wp-content/conference-presentations/2020/2020-w1-d2-m1-JD-SynCOR.pdf, accessed June 5, 2024.
45 Z. Haonan, Z. Cunquan, Z. Meng and S. Peng-cheng, *Cryogenics*, 2020, **106**, 103022.
46 K. Bhagaloo, R. Ali, A. Baboolal and K. Ward, *Sustain. Energy Technol. Assessments*, 2022, **51**, 101910.
47 M. Temkin and V. Pyzhev, *J. Phys. Chem.*, 1939, **13**, 851–857.
48 Methanex, Pricing, https://www.methanex.com/about-methanol/pricing/, accessed July 12, 2024.
49 B. Analytiq, Ammonia Price Index, https://businessanalytiq.com/procurementanalytics/index/ammonia-price-index/, accessed July 5, 2024.
50 W. N. Association, Heat Values of Various Fuels, https://world-nuclear.org/information-library/facts-and-figures/heat-values-of-various-fuels, accessed July 4, 2024.
51 L. Eggemann, N. Escobar, R. Peters, P. Burauel and D. Stolten, *J. Clean. Prod.*, 2020, **271**, 122476.
52 C. Zamfirescu and I. Dincer, *J. Power Sources*, 2008, **185**, 459–465.
53 M. A. J. Huijbregts, Z. J. N. Steinmann, P. M. F. Elshout, G. Stam, F. Verones, M. Vieira, M. Zijp, A. Hollander and R. van Zelm, *Int. J. Life Cycle Assess.*, 2017, **22**, 138–147.
54 P. Nikolaidis and A. Poullikkas, *Renew. Sustain. Energy Rev.*, 2017, **67**, 597–611.
55 M. Demartini, F. Tonelli and K. Govindan, *Cleaner Logistics and Supply Chain*, 2022, **3**, 100020.